DRAFT
CMS Paper

The content of this note is intended for CMS internal use and distribution only

Time-integrated mixing probability for B mesons

The CMS Collaboration

Abstract

A measurement of the integrated mixing probability for neutral B mesons $\bar{\chi}$ is presented, based on a data sample corresponding to an integrated luminosity of 27.9 pb^{-1} collected by the CMS experiment at the LHC at $\sqrt{s} = 7$ TeV. Pairs of muons are selected, where each particle has momentum $p_{\mathrm{T}} > 4$ GeV and pseudorapidity $|\eta| < 2.1$. By comparing the amount of equal charge combinations to the overall number of pairs, the value $\bar{\chi} = 0.134 \pm 0.001(\text{stat.}) \pm ?(\text{syst})$ is obtained. This result is used to constrain the probabilities for the hadronization of a b-quark to either a B^0 or B_s meson.

This box is only visible in draft mode. Please make sure the values below make sense.

PDFAuthor:	Mario Galanti,Martino Margoni,Luca Perrozzi,Nicola Pozzobon,Franco Simonetto
PDFTitle:	Time-integrated mixing probability for B mesons
PDFSubject:	CMS
PDFKeywords:	CMS, physics, software, computing

Please also verify that the abstract does not use any user defined symbols

1 Introduction

Flavor changing neutral currents induce the flavor (F) transformation $\Delta F = 2$ of a neutral B-meson into its antiparticle and viceversa. In the standard model this phenomenon is described by box diagrams involving the exchange of two up-like quarks (mostly top) and two W bosons. Precise measurements of the flavor oscillation frequencies, $\Delta m_d = 0.508 \pm 0.003$ (stat) ± 0.003 (syst) ps^{-1} and $\Delta m_s = 17.77 \pm 0.10$ (stat) ± 0.07 (syst) ps^{-1} have been performed for B^0 mesons by the B-factories [1 **? ?**], and for B_s mesons by the CDF collaboration [**?**]. The corresponding time integrated mixing probabilities, $\chi_d = \frac{\Gamma(b \to B^0 \to \bar{B}^0)}{\Gamma(b \to B^0)} = 0.1873 \pm 0.0024$ and $\chi_s = 0.49927 \pm 0.00003$ are computed by integrating the functions describing the time dependent B-flavor oscillation.

A measurement of the average time integrated mixing probability, $\bar{\chi} = \frac{\Gamma(b \to B \to \bar{B})}{\Gamma(b \to B)} = f_d \chi_d + f_s \chi_s$ (charge conjugate processes are always implied) with the CMS detector at the LHC is described here, where f_d and f_s are the fractions of B^0 and B_s mesons in an unbiased sample of weakly decaying b-hadrons. The measurement of $\bar{\chi}$ provides therefore a constraint on the values of f_d and f_s. Uncertainties on the b-sample composition are among the largest sources of systematic errors in the measurements of b-hadrons branching fractions at LHC [**?**].

Experimentally, $\bar{\chi}$ is measured by comparing the rates of events with two equal or opposite charge leptons from the semileptonic decay $B \to \ell^+ \nu_\ell X$. Same-charge events occur when one, and one only, of the two B-hadrons produced undergoes mixing (hereafter, mixed events). Opposite-charge data (herefater, unmixed) are observed when either none or both the mesons have oscillated. Precise measurements of $\bar{\chi}$ have been performed by the LEP collaborations [**? ? ? ?**] in $e^+ e^-$ collisions at $\sqrt{s} = 91$ GeV. The LEP average $\bar{\chi} = 0.126 \pm 0.004$ [**?**] is still the most precise determination of $\bar{\chi}$. The latest CDF result $\bar{\chi} = 0.126 \pm 0.008$ [**?**] is well consistent with the LEP value, conferming the hypothesis that B-hadrons are produced in equal proportions in $e^+ e^-$ and $p\bar{p}$ colliders. It should be noted that, to derive this result, a sizable fraction of the CDF dimuon sample is assigned to an unknown origin, not explained by standard model sources [**?**] .

It is not expected a priori that the B-hadron sample composition at the LHC be the same as at LEP or Tevatron, because the intial state in a pp collision is not flavor symmetric, with four valence u-quarks and two valence d-quarks. The LHCb collaboration has measured the composition of the B-hadron mixture by comparing the event rates in fully reconstructed final states [**?**]. These measurements are however performed in a different kinematical domain, and are intrinsically limited by the knowledge of the branching ratios of the reference B decays. A measurement of $\bar{\chi}$ at CMS allows therefore a comparison with the results obtained at flavor symmetric colliders or in a different kinematic range at LHC. Besides increasing our understanding of the $b \to B$ fragmentation process, this helps improving the measurements of rare B decays from the LHC experiments.

Events are selected containing at least two muons, each with $p_T > 4$ GeV and $|\eta| < 2.1$, where p_T is the projection of the track momentum in the direction orthogonal to the beam axis, and the pseudorapidity $\eta = -\ln[\tan(\theta/2)]$ is defined from the angle θ between the track momentum and the counterclockwise beam direction. Each muon must belong to a jet reconstructed with a particle flow algorithm. The momentum of the muon in the direction ortogonal to the jet axis, p_T^{jet}, is used to discriminate signal events from the background, which includes muons from c and light hadrons decays, punch through and muons from the cascade process $B \to \bar{D} X \to \ell^- \bar{\nu}_\ell X'$. This last source results in muons with the opposite charge correlation to the original B meson flavor as compared to the signal, diluting the sensitivity of the measurement.

To improve background rejection the muon is removed from the jet when computing the jet axis direction. The signal fractions in the mixed and unmixed samples are determined with a two-dimensional (2D) fit to the muons p_T^{jet}.

The measurement is performed first on the full selected sample. Then events are separated into three sets, depending on whether the impact parameters d_{xy} of the two muons are both below a given threshold, both above the threshold, or one below and one above. The impact parameter, defined as the distance of minimal approach of the muon track to the collision point, projected in the plane ortogonal to the beam direction, is a good estimator of the proper decay time of the B hadron. Due to the much larger oscillation frequency, B_s contributes more to mixing in the low d_{xy} region, whereas the high d_{xy} sample contains a significant fraction of events from B^0 mixing. Finally, the measurements are repeated separately for positive-charge and negative-charge mixed events.

This paper is structured as follows. A brief description of the CMS detector is presented in Section 2. Section 3 describes the collision and simulated data used for this measurement and the selection criteria. Section 4 contains a detailed description of the categories in which events are grouped according to each muon's production process and kinematic features, while the fit to the p_T^{jet} distributions is discussed in Section 5. Section 6 is devoted to the determination of the systematic uncertainties. Section **??** summarizes the results.

2 The CMS detector

A detailed description of the CMS experiment can be found elsewhere [2]. The central feature of the CMS apparatus is a superconducting 3.8 T solenoid of 6 m internal diameter. Within the field volume are the silicon tracker, the crystal electromagnetic calorimeter (ECAL), and the brass/scintillator hadron calorimeter (HCAL). Muons are detected in the pseudorapidity range $|\eta| < 2.4$ by gaseous detectors utilizing three technologies: drift tubes (DT), cathode strip chambers (CSC), and resistive plate chambers (RPC), embedded in the steel return yoke. The silicon tracker is composed of pixel detectors (three barrel layers and two forward disks on either side of the detector, made of 66 million $100\,\mu m \times 150\,\mu m$ pixels) followed by microstrip detectors (ten barrel layers, three inner disks and nine forward disks on either side of the detector, with the strip pitch between 80 and $180\,\mu m$). Thanks to the strong magnetic field and high granularity of the silicon tracker, the transverse momentum p_T of muons matched to reconstructed tracks is measured with the resolution better than 1.5% for $p_T < 100\,GeV$. The silicon tracker also provides the vertex position with $\sim 15\,\mu m$ accuracy. The impact parameter resolution is measured with a sample of muons from $Y(1S) \rightarrow \mu^+\mu^-$ decays to be $28\,\mu m$ for muons with $p_T > 4\,GeV$.

The first level (L1) of the CMS trigger system, composed of custom hardware processors, uses information from the calorimeters and muon detectors to select the most interesting events. The rapidity coverage of the L1 muon triggers used in this analysis is $|\eta| < 2.4$. The high-level-trigger processor farm further decreases the event rate before data storage.

3 Data selection and Monte Carlo simulation

The data employed for this measurement were collected with the CMS detector during the 2010 running period of the LHC. They correspond to an integrated luminosity $\mathcal{L} = 27.9 \pm 1.1\,pb^{-1}$ [3]. A sample of events with two muons, each with transverse momentum $p_T > 3\,GeV$ were selected at the trigger level. Further requirements, designed to increase the purity of the

muon candidates and to increase the fraction of muons from b decay in the sample, are applied at the analysis stage. A muon candidate is selected by matching information from the silicon tracker and muon chambers. The track must contain at least 12 hits from the silicon tracker, with signals in at least two pixel layers, and a normalized χ^2 not exceeding 2. The overall χ^2 obtained by combining the information from the tracker and the muon chambers should not exceed 10 times the number of degrees of freedom. Finally, each muon must be contained in the kinematical region defined by $|\eta| < 2.1$ and $p_\text{T} > 4\,\text{GeV}$.

Primary interaction vertices are reconstructed event-by-event from the reconstructed tracks. A candidate vertex is accepted if its fit has at least four degrees of freedom and its distance from the beam spot does not exceed 24 cm along the beam line and 1.8 cm in the plane transverse to the beams. Tracks are assigned to the primary vertex for which the track's distance to the vertex along the beam direction is smallest at the point of closest approach in the transverse plane. Muon tracks are required to have an impact parameter d_{xy} perpendicular to the beam direction and with respect to its assigned primary vertex of less than 0.2 cm. Events are kept only if both muon tracks are assigned to the same primary vertex, and both cross the beam axis within 1 cm of that vertex position along the beam direction.

Jets are reconstructed with a particle flow technique combining information from the tracker, the calorimeters and the muon chamber. The anti-K_T algorithm is employed, with a cone selection of ... Jets with $p_\text{T} < 10\,\text{GeV}$ are rejected. Muons not associated to a selected jet are then neglected. The muon momentum in the direction perpendicular to the jet axis, p_T^{jet}, is then computed. To increase the discriminant power of this variable, the muon 3-momentum is first subtracted from the jet. If less than two muons associated to different jets are found, the event is rejected.

The dimuon invariant mass must be contained in the range $5\,\text{GeV} < M_{\mu\mu} < 70\,\text{GeV}$. The lower bound rejects events from charmonium resonances and sequential semileptonic decays from a single b quark (for example $b \rightarrow J/\psi\, X \rightarrow \mu\mu X$, or $b \rightarrow c\mu X \rightarrow \mu\mu X'$), the upper bound removes events from Z^0 decays.

If more than one muon pair is selected in an event, the combination with the largest values of p_T^{jet} is used. A total of ... are finally selected.

A sample of simulated Monte Carlo (MC) events were generated using the minimum-bias settings of PYTHIA 6.422 [4] (parameter MSEL=1), with the Z2 tune [5], and incorporating the CTEQ6L1 parton distribution functions (PDF) [6]. To increase the generation efficiency within the selected acceptance, a filter was applied at the generator level requiring two muons with $p_\text{T}^\text{gen} > 2.5\,\text{GeV}$ and $|\eta^\text{gen}| < 2.5$. The generated samples include events with muons originating from the decay of light mesons (mostly charged pions and kaons) within the tracker volume.

A third MC sample was produced to simulate the Drell–Yan process. MC events, including the full simulation of the CMS detector and trigger via the GEANT4 package [7], are subjected to the same reconstruction and selection as the real data.

4 Templates for different muon classes

The fraction of signal events in each data sample is obtained from a fit to the 2D distribution of the p_T^{jet} of the two muons. For this purpose, reconstructed muons in the simulated events are separated into different classes, defined according to their origin. The single-particle p_T^{jet}

distributions are obtained for each class from simulation and fitted using analytical functions. From these functions, the 2D templates are built symmetrically. This procedure is described in the following section.

4.1 Definition of muon classes

Information from the generation process is used to assign each reconstructed muon in the simulation to a well-defined category. Reconstructed muon candidates are linked to the corresponding generated charged particles with a hit-based associator, which reduces the probability of incorrect associations to a negligible level. Tracks are assigned to one of the following classes:

1. primary B decays (*bP*), corresponding to muons produced in the semileptonic decay of a *B* hadron, b $\rightarrow \mu^- X$.

2. sequential B decays (*bS*), where the muon comes from the semileptonic decay of a charm hadron or the leptonic decay of a tau lepton produced in the B-hadron decay;

3. uncorrelated background muons (*bkg*). This class includes those produced from leptonic or semileptonic decays of promptly produced charm hadrons, of charged pions and kaons, from charmonium states, and long lived hadrons punching through the calorimeters up to the muon chambers.

For events in class (1), the charge of the muon track tags the flavor of the parent b-quark at decay time: a negative-charge muon is produced from the decay of an hadron containing a b-quark, a positive-charge muon flags a $\bar{\text{b}}$-quark. Most of the muons in class (2) are produced in the cascade process b $\rightarrow$ cX $\rightarrow \mu^+ X'$ with the reverse charge-flavor correlation, diluting the sensitivity of the measurement (Wrong Charge *bS* decays). The same correlation as for the signal is found instead if either the muon comes from a tau lepton, b $\rightarrow \tau^- X \rightarrow \mu^- X'$, or from a charm hadron produced from the virtual W^* boson in double charm B-decays b $\rightarrow$ cW^{*-} $\rightarrow$ c$\bar{c}$X $\rightarrow \mu^- X'$.

The charge of class (3) muons does not convey any information on b-quark flavor.

Table 1 gives the single-muon sample composition from the simulation for MC events passing the full selection, including trigger. The predicted composition of the dimuon events from the

Table 1: Percentage of each muon class in the simulated events. The uncertainties are statistical only.

Source	Fraction in simulation (%)
Primary B (*bP*)	59.8 ± 0.1
Sequential B decays (*bS*)	12.4 ± 0.2
Random Background (*bkg*)	27.8 ± 0.1

simulation is shown in Table 2, grouped on the basis of the charge correlation. The uncertainties given in the tables are the statistical uncertainties from the simulated samples.

The shape of the muon p_T^{jet} spectrum is determined by the production and decay properties of the parent hadron. Primary B decays are neatly separated from the rest due to the larger mass and harder fragmentation of b-quarks. A slight separation in observed between sequential B decays and uncorrelated background. The spectra from Good Charge and Wrong Charge *bS* decays are identical. Fig.1 shows the template histograms obtained in the simulation for the three classes.

Table 2: Percentage of dimuon event sources in the simulation. Events from B-decays are classified as GC and WC on the basis of the correlation betweeen the muon charge and the b-quark flavor.

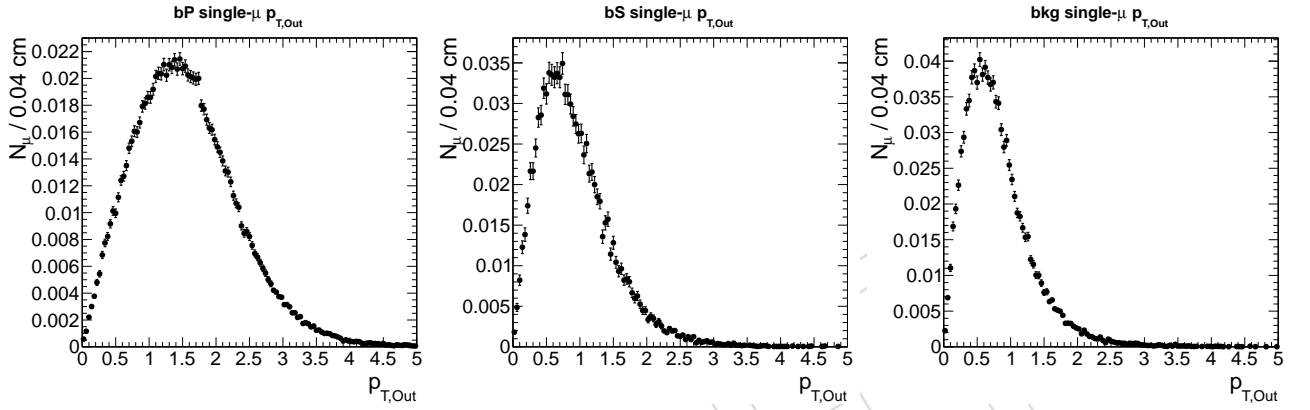| Source	Fraction in simulation (%)
GC-GC	60.1 ± 0.2
GC-WC	5.0 ± 0.1
GC-*bkg*	13.5 ± 0.1
WC-WC	0.1 ± 0.1
WC-*bkg*	0.6 ± 0.1
bkg-bkg	20.7 ± 0.1

Figure 1: 1D p_T^{jet} distributions for the different categories. Left: B hadron direct decays (bP), center: B hadron sequential decays (bS), right: hadrons containing light quarks decays (*bkg*).

4.2 Two-dimensional template distributions

In principle, nine two-dimensional (2D) distributions should be obtained combining the three one-dimensional (1D) templates defined above. In order to reduce the number of categories, the p_T^{jet} distributions are symmetrized (i.e. *bP-bkg=bkg-bP*, etc.) using a method originally developed by the CDF collaboration [8], and already used by CMS for the measurement of the $b\bar{b}$ production cross section in pp collisions at $\sqrt{s} = 7$ TeV [?]. The 1D histograms, built as described above, are normalized to unity within the fit range $0 < p_T^{jet} < 5$ GeV. The symmetrized 2D template histogram for the events with a muon of class ρ and another of class σ (ρ, $\sigma = 1, 2, 3$ according to the definition in Section 4.1) is then constructed as:

$$T_{ij}^{\rho\sigma} = \frac{1}{2}(S_i^\rho S_j^\sigma + S_j^\rho S_i^\sigma), \tag{1}$$

where S_i^ρ is the content of the ith bin of the histogram describing the class ρ, and analogously for index j and class σ. In this way six symmetric distributions are obtained. The 1D projections of the corresponding templates are shown in Fig. 2.

5 Measurement of $\bar{\chi}$

Consistent with the symmetric 2D templates, the data events are also randomized by taking the p_T^{jet} of the two muons in each event, and filling the bin corresponding to $[p_T^{jet}(\mu_1), p_T^{jet}(\mu_2)]$ or to $[p_T^{jet}(\mu_2), p_T^{jet}(\mu_1)]$ according to the outcome of a random number generator. Events where
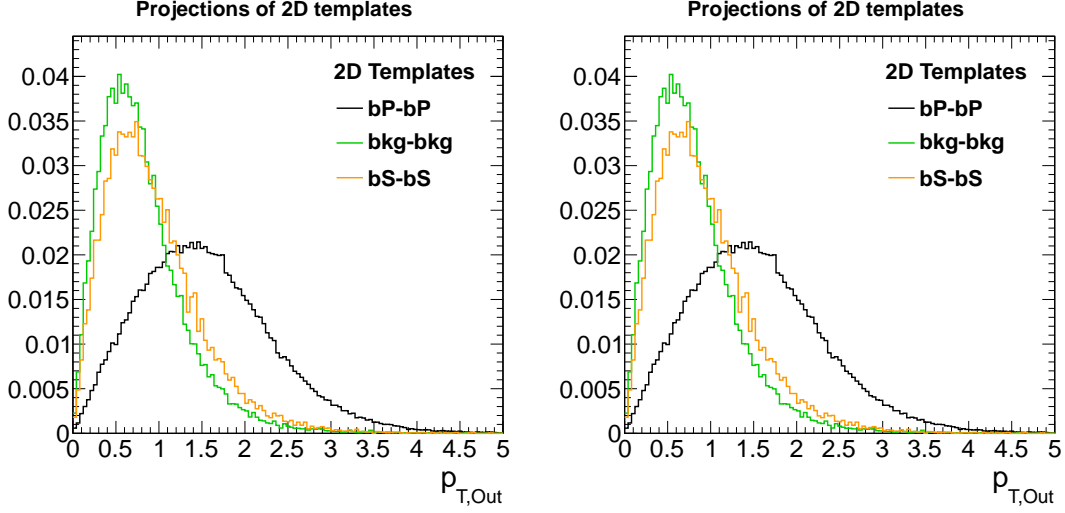
Figure 2: 1D projections of the p_T^{jet} 2D templates used in the fit for *bP-bP bS-bS* (bottom left), *bkg-bkg* on the left, and *bP-bS bP-bkg bS-bkg* on the right.

the two muons have the same electric charge are collected in the Like-Charge (LC) sample, the others in the Opposite-Charge (OC) sample. The amount of events from different sources in each sample is determined with a two dimensional (2D) binned maximum-likelihood fit. The fit minimizes the function:

$$-2 \cdot \ln(L) = -2 \left\{ \sum_{i,j=1} \left[n_{ij}\ln(\nu_{ij}) - \nu_{ij} \right] - \frac{1}{2} \sum_{k'=1}^{3} \left(\frac{r_{k'} - r_{k'}^{MC}}{\sigma_{r_{k'}}^{MC}} \right)^2 \right\}, \qquad (2)$$

where n_{ij} is the content of the data histogram in the bin (i, j), $\nu_{ij} = \Sigma_{\rho,\sigma} f_{\rho,\sigma} T_{i,j}^{\rho,\sigma}$, $f_{\rho,\sigma}$ is the parameter expressing the number of events from the $T^{\rho,\sigma}$ template ($\rho = 1, 3, \sigma = 1, \rho$). In principle six parameters must be determined in each of the two fits. To reduce the number of fit parameters and ease the fit convergence, the three parameters $f_{,}$, $f_{bkg,bkg}$, and $f_{bS,bkg}$ are constrained so that the ratios $f_{bS,bS}/f_{bP,bP}$, $f_{bkg,bkg}/f_{bP,bkg}$, and $f_{bS,bkg}/f_{bP,bS}$ are compatible with the MC expectations within their statistical uncertainties. In Eq. (2), k is the index of the constrained templates (*bSbS*, *bkgbkg*, and *bSbkg*) r_k is the ratio of the constrained fit fraction with respect to the reference fit fraction (for instance in the *bSbS* case $r_{bS,bS} = f_{bS,bS}/f_{bP,bP}$), r_k^{MC} is the ratio of the constrained fraction and reference fraction in the simulation, and $\sigma_{r_k}^{MC}$ its statistical uncertainty from the number of simulated events.

Tab. 3 gives the results of the fit to the LC and OC data samples. The quoted uncertainties are obtained from the fit and are statistical only.

Projections of the p_T^{jet} distributions with the results of the fits are shown in Fig. 3.

Figure 3: Top: The projected d_{xy} distributions from data with the results of the fit for muons with $p_T > 4\,\text{GeV}$ (left) and $p_T > 6\,\text{GeV}$ (right). The distribution from each dimuon source is shown by the histograms. Bottom: The pull distribution from the fit.

Table 3: Results of the likelihood fit to data.

Parameter	
$N_{b\bar{b}}$	
$N_{bkg|bkg}^{LC}$	
$N_{bkg|bkg}^{OC}$	
$N_{b\bar{b}|bkg}^{LC}$	
$N_{b\bar{b}|bkg}^{OC}$	
f_{bW}	
$\bar{\chi}$	

Table 4: Statistical correlation of the fit parametrs with $\bar{\chi}$

Parameter	f_{bW}	$N_{b\bar{b}}$	$N_{b\bar{b}|bkg}^{LC}$	$N_{b\bar{b}|bkg}^{OC}$	$N_{bkg|bkg}^{LC}$	$N_{bkg|bkg}^{OC}$
Correlation	0	0	0	0	0	0

6 Systematic uncertainties

Several sources of systematic uncertainties have been considered for this measurement. They are divided into uncertainties due to the model dependencies for both the signal and the backgrounds, experimental effects affecting the p_T^{jet} definition, and the fit method. Each of these is described separately in the subsections below.

6.1 Model-dependent uncertainties

Analysis bias: the value of $\bar{\chi}$ depends on the composition of the weakly-decaying B-hadrons after hadronization. The mixture observed in the MC after all selection requirements are applied is consistent with that at the generation phase. The statistical uncertainty of this comparison is propagated to the systematic uncertainty on $\bar{\chi}$.

B hadron composition: differences in the masses of the weakly decaying heavy hadrons might affect the p_T^{jet} distributions. The b and c-hadron sample compositions are varied by the errors of the LEP measurements, p_T^{jet} templates are recomputed and the fit is repeated. The variation on the result is added in quadrature to the systematic uncertainty.

Sequential B decays: the contribution from bW decays is determined by the fit, while the less sizeable bG contribution is constrained to that result by the r_{GW} factor. The systematic uncertainty is computed by varying the branching fractions for $b \rightarrow \tau X$, $b \rightarrow D\bar{D}X$, and $b \rightarrow DX$ by their errors [**?**], and repeating the fit with the recomputed values of r_{GW}.

b-quark fragmentation: uncertainties in the production of B hadrons from the fragmentation of a b quark affect the shape of the p_T^{jet} distributions. The systematic uncertainty is computed as the difference between the default result and those obtained with two different hadronization models in the PYTHIA simulation: the Lund symmetric [4] and the Peterson [9] functions *da ridiscutere: pare che sia meglio un'altra parametrizzazione.*

Heavy Flavor decays : PYTHIA default generator is used to describe the semileptonic decays of beauty and charm hadrons. MC events are then weighted to reproduce the spectra measured at the B-factories, described by the EVTGEN Monte Carlo. Templates are recomputed and the fit is repeated. The difference with the default result is the systematic uncertainty.

229 *Light-meson decays in flight:* muons from π and K decays have different p_T^{jet} distributions. The
230 shape is also different for muons from light mesons produced in the hadronization of a light
231 quark, or from the decay of a heavy hadron. The relative amount of high-p_T pion to kaon
232 tracks is varied in a range of $\pm$%, consistent with the precision of CMS measurments [**?**], [**?**
233]. Likewise, the fraction of light mesons from light quarks or from heavy flavors is varied by
234 $\pm$%, corresponding to the uncertainties on the measurements of heavy flavor production at the
235 LHC [**?**],[**?**],[**?**],[**?**].

236 The generator-level filter applied to the simulated sample, requiring two muons to be produced
237 within the tracker volume in each event, affects the shape and composition of the decays-in-
238 flight template. The impact of the filter on the BB fraction is estimated by extracting the decays-
239 in-flight template from an unbiased simulated sample in which only one generated muon is
240 required to pass the filter and the other muon is used in determining the template. Repeating
241 the analysis with this new template results in a ?? variation for $\bar{\chi}$.

242 The total model-dependent systematic uncertainty, found by adding in quadrature the contri-
243 butions listed above, is .

6.2   Experimental uncertainties in p_T^{jet} determination

245 Jets are reconstructed with a particle flow algorithm which exploits at best the detector in-
246 formation. Difference in the resolution in data and simulation affect the definition of the jet
247 direction, and therefore the p_T^{jet} templates. The resolution is measured both in data and in
248 MC using a subset of events where a secondary vertex can be reconstructed from the charged
249 tracks contained in the jet. The vertex must be formed by at least three tracks, and the distance
250 in space between its position and that of the nearest primary vertex must exceed N times the
251 error. In this very pure sample of events from B-decay, the vector joining the primary vertex
252 to the secondary vertex positions is used to determine the azimuthal and polar coordinates of
253 the decaying B-hadron with great precision. They are then compared to those obtained inde-
254 pendently from the jet direction. The RMS azymuthal resolution is $\Delta\phi = \sigma(\phi_{jet} - \phi_{vertex}) = ...$
255 rad in the data, and ... in the MC. For the polar angle the resolution is $\Delta\theta = ...$ in data and ... in
256 the MC.

6.3   Uncertainties related to the Monte Carlo precision and the fit method

258 There are three general categories of systematic uncertainty caused by the MC statistical preci-
259 sion and the fitting procedure. These include:

260 *Monte Carlo precision:* the likelihood fit is validated using a set of 500 parameterized simulated
261 datasets, each with the same number of events as the data sample. The fit results from these
262 datasets reproduce the input values with uncertainties consistent with those obtained in data,
263 and the pull distribution is well described by a normal function. The r.m.s. of the results ob-
264 tained for $\bar{\chi}$ ....%, is taken as the systematic uncertainty related to the finite simulated sample.

265 *Template parameterization:* the distributions in the simulated data used for the fit are smoothed
266 using a superposition of a ???? . The associated systematic uncertainty, evaluated by using dif-
267 ferent parametrizations, is equal to ... The systematic uncertainty from the use of symmetrized
268 templates is estimated to be ... by comparing the results obtained in the simulation when a sum
269 of symmetrized templates is used as pseudo-data instead of the usual randomized distribution.

270 *Bin size and fit upper bound:* varying the bin size in the range ... accounts for a systematic
271 uncertainty of .... while varying the fit upper bound in the range ... accounts for ...

The total systematic uncertainty related to the fit method is found by adding the contributions in quadrature, which gives ...

6.4 Overall systematic uncertainty

All the systematic uncertainties described so far are summarized in Table 5 and sum in quadrature to ..., with the larger contribution coming from ... For sake of completeness, Table 5 reports also the breakdown of the systematic uncertainties affecting the measurement of f_{bW} which is another significant physical parameter. Table 6 reports the correlation of the other fitted parameters with $\bar{\chi}$, including the systematic uncertainties.

Table 5: Systematic uncertainties on the measurements of $\bar{\chi}$ and of f_{bW}

Source	$\bar{\chi}$	f_{bW}
Model dependency		
Jet definition		
Monte Carlo precision and fit method		
Total		

Table 6: Correlation, including statistical and systematic uncertainties, of the fit parametrs with $\bar{\chi}$

Parameter	f_{bW}	$N_{b\bar{b}}$	$N_{b\bar{b}|bkg}^{LC}$	$N_{b\bar{b}|bkg}^{OC}$	$N_{bkg|bkg}^{LC}$	$N_{bkg|bkg}^{OC}$
Correlation	0	0	0	0	0	0

References

[1] Heavy Flavour Averaging Group (HFAG) Collaboration, "Averages of b-hadron, c-hadron, and tau-lepton Properties", (2010). arXiv:1010.1589.

[2] CMS Collaboration, "The CMS experiment at the CERN LHC", *JINST* **03** (2008) S08004. doi:10.1088/1748-0221/3/08/S08004.

[3] CMS Collaboration, "Measurement of CMS Luminosity", CMS Physics Analysis Summary CMS-PAS-EWK-10-004, (2010).

[4] T. Sjöstrand, S. Mrenna, and P. Skands, "PYTHIA 6.4 physics and manual", *JHEP* **05** (2006) 026. doi:10.1088/1126-6708/2006/05/026.

[5] R. Field, "Early LHC Underlying Event Data–Findings and Surprises", in *Proceedings of the Hadron Collider Physics Symposium 2010*. 2010. arXiv:1010.3558.

[6] J. Pumplin et al., "New Generation of Parton Distributions with Uncertainties from Global QCD Analysis", *JHEP* **07** (2002) 012. doi:10.1088/1126-6708/2002/07/012.

[7] GEANT4 Collaboration, "GEANT4–a Simulation Toolkit", *Nucl. Instr. Meth. A* **506** (2003) 250. doi:10.1016/S0168-9002(03)01368-8.

[8] CDF Collaboration, "Measurement of correlated $b\bar{b}$ production in $p\bar{p}$ collisions at $\sqrt{s} =$1960 GeV", *Phys. Rev. D* **77** (2008) 072004. doi:10.1103/PhysRevD.77.072004.

[9] C. Peterson et al., "Scaling violations in inclusive e^+e^- annihilation spectra", *Phys. Rev. D* **27** (1983) 105. doi:10.1103/PhysRevD.27.105.